Dissociation of One-Dimensional Matter-Wave Breathers due to Quantum Many-Body Effects

Vladimir A. Yurovsky, Boris A. Malomed, Randall G. Hulet, and Maxim Olshanii

Phys. Rev. Lett. **119**, 220401 — Published 28 November 2017

DOI: 10.1103/PhysRevLett.119.220401

Dissociation of one-dimensional matter-wave breathers due to quantum many-body effects

Vladimir A. Yurovsky,[1] Boris A. Malomed,[2,3] Randall G. Hulet,[4] and Maxim Olshanii[5]

[1] *School of Chemistry, Tel Aviv University, 6997801 Tel Aviv, Israel**
[2] *Department of Physical Electronics, School of Electrical Engineering, Faculty of Engineering, Tel Aviv University, Tel Aviv 6997801, Israel*
[3] *ITMO University, St. Petersburg 197101, Russia*
[4] *Department of Physics and Astronomy, Rice University, Houston, TX 77005, USA*
[5] *Department of Physics, University of Massachusetts Boston, Boston, MA 02125, USA*

We use the ab initio Bethe Ansatz dynamics to predict the dissociation of one-dimensional cold-atom breathers that are created by a quench from a fundamental soliton. We find that the dissociation is a robust quantum many-body effect, while in the mean-field (MF) limit the dissociation is forbidden by the integrability of the underlying nonlinear Schrödinger equation. The analysis demonstrates the possibility to observe quantum many-body effects without leaving the MF range of experimental parameters. We find that the dissociation time is of the order of a few seconds for a typical atomic-soliton setting.

Under normal conditions, interacting quantum Bose gases do not readily exhibit signatures of their corpuscular nature, but rather follow the behavior predicted by mean-field (MF) theory. The observability of microscopic quantum effects involving a substantial fraction of the particles in a coherent macroscopic setting generally requires going beyond-MF, for example, in low density in 1D [1, 2] or high density in 3D. In 3D systems, the high-density Lee-Huang-Yang corrections, which are induced by quantum correlations, were realized experimentally using the Feshbach resonance [3] and in the spectacular form of "quantum droplets" in dipolar [4–6] and isotropic [7] bosonic gases., i.e., as self-trapped states stabilized against the collapse by the beyond-MF self-repulsion. This stabilization was predicted in Refs. [8–10]. Quantum effects involving a macroscopic number of atoms in collapsing attractive 3D gases and colliding condensates were also observed [11–15] and analyzed [16, 17] in the MF density range.

A generic opportunity to observe beyond-MF effects arises when a particular symmetry of the MF dynamics, which prohibits a certain effect, is broken at the microscopic level thus making observation of the effect possible. For instance, the scale invariance in the dynamics of a harmonically trapped 2D Bose gas nullifies the interaction-induced shift of the frequency of monopole excitations for all excitation amplitudes; however, this scale invariance is broken by the quantum many-body Hamiltonian, leading to a small shift, albeit discernible on a zero background [18]. In this context, the symmetry breaking by the secondary quantization may be considered as a manifestation of a general phenomenon known as the quantum anomaly [19]. In this Letter we develop a similar strategy for predicting beyond-MF effects in the one-dimensional (1D) self-attractive Bose gas in an MF range of parameters. The respective MF equation amounts to the nonlinear Schrödinger (NLS) equation, integrable by the inverse-scattering transform [20]. The NLS rigidly links the structure of a time-dependent solution to its initial form, with many features of the latter rendered identifiable in the former. In particular, a sudden increase of the strength of the attractive coupling constant by a factor of 4, i.e. an interaction *quench*, converts a fundamental soliton into an exact superposition of two solitons with zero relative velocity, zero spatial separation, and with a mass ratio $3:1$ [21–23]. The two superimposed solitons have different chemical potentials, hence the density oscillates as a result of interference. Such an exact superposition of fundamental solitons is identified as an NLS breather.

Further, quantum fluctuations in solitons have also been analyzed in terms of the exact Bethe-ansatz (BA) solution [24–27], the linearization approximation [28], and the numerical positive-P representation [29, 30]. These effects have been observed in experiments [31–34], see also review [35]. In particular, in the quantum many-body theory, contrary to its MF counterpart, the center-of-mass (COM) position of a soliton is a quantum coordinate whose conjugate momentum is subject to quantum fluctuations [36–38].

The MF breather generated by the quench does not split due to the absence of any relative velocity in the MF. We predict, however, that the spread of the relative velocity of the two solitons leads to dissociation, and thus reveals a many-body quantum effect.

In Ref. [39] it is shown, using a Bose-Hubbard model, that higher-order solitons also break up due to many-body quantum effects. The fact that a nonintegrable lattice model, with thermalization of eigenstates, also predicts many-body quantum effects is relevant for comparison with results of the present work.

We consider N atoms of mass m moving in a waveguide with a transverse trapping frequency $\omega_\perp$. In the "deep 1D" approximation they can be considered as particles moving in the x direction, with zero-range interactions of strength $g = 2\hbar a\omega_\perp$ [40], where the s-wave scattering

length a can be tuned by an external magnetic field via the Feshbach resonance. The corresponding Lieb-Liniger Hamiltonian is [41]

$$\hat{H} = -\frac{\hbar^2}{2m}\sum_{j=1}^{N}\frac{\partial^2}{\partial x_j^2} + g\sum_{j<j'}\delta(x_j - x_{j'}) \ . \qquad (1)$$

This problem has an exact BA solution [24, 42]. Due to the translational invariance of the Hamiltonian (1), its eigenfunctions are delocalized, having a homogeneous density. For attractive interactions with $g < 0$, there are also eigenstates in the form of one or several several strings – bound states of several particles, i.e., quantum solitons [24, 25, 43]. Although they remained a theoretical concept since they were introduced, very recently similar states — the Bethe strings — have been directly observed in an antiferromagnetic Heisenberg-Ising chain [44]). A superposition of strings with different velocities may remain localized for a finite time, so that it carries over into an MF multi-soliton (breather) in the limit of $N \to \infty$ [26–28]. Normalization factors for multi-string states were derived in Ref. [45].

We assume that, at $t < 0$, the interaction strength was $g_0 = g/4$, and the system contained a single-string state $\varphi_N^{(0)}$ with zero COM velocity. At $t = 0$, the external magnetic field suddenly changes, switching the interaction strength to g, i.e., applying a 4-fold *quench* to the system. The exact BA calculation, starting from the quenched state, makes it possible to directly compare the result in the quantum many-body system with its exactly known MF counterpart — the second-order breather, which is generated by the 4-fold quench [22]. This is, essentially, the objective of the present work.

After the application of the quench, the many-body configuration will be a superposition of a single-string state φ_N, double-string states $\varphi_{N_1,N-N_1,v}$, where v is the relative velocity of two strings composed of N_1 and $N - N_1$ atoms, and multi-string states. On the other hand, a fundamental quantum soliton is a superposition of the single-string states with different COM velocities. These states are mutually orthogonal due to the COM velocity conservation, therefore probabilities of quench-triggered transitions from the pre-quench fundamental-soliton state to multi-soliton ones will be the same as for the delocalized string states. The probabilities are calculated analytically using the exact BA solution [46]. It is the basic technical result of the present work, which underlies the physical considerations. First, the probability to remain in the single-string state is

$$\left|\left\langle \varphi_N^{(0)}|\varphi_N\right\rangle\right|^2 = \left(\frac{2\sqrt{|gg_0|}}{|g|+|g_0|}\right)^{2(N-1)} = \left(\frac{4}{5}\right)^{2(N-1)}$$

For the double-string states the probabilities depend on the relative string velocity $v > 0$ and the string composition,

$$\frac{dP_{N_1,N-N_1}(v)}{dv} = (2-\delta_{N_1,N-N_1})\left|\left\langle \varphi_N^{(0)}|\varphi_{N_1,N-N_1,v}\right\rangle\right|^2 . \qquad (2)$$

It is a sum of the probabilities corresponding to velocities v and $-v$ for $N_1 \neq N-N_1$, while for $N_1 = N/2$ the states with v and $-v$ are identical. Examples of the probabilities are displayed in Fig. 1, for $N = 4$ and $N = 20$. The natural velocity scale is

$$v_0 = |g|/(2\hbar) \equiv a\omega_\perp \qquad (3)$$

Total probabilities of the transition to double-string states with fixed N_1,

$$P_{N_1} \equiv \int_0^\infty \frac{dP_{N_1,N-N_1}(v)}{dv}dv, \qquad (4)$$

are presented in Fig. 2 making it obvious that the transition $N \to 3N/4 + N/4$ features the *largest probability*, in agreement with the MF prediction. The cumulative probability of the transition to all double-string states, $\sum_{N_1=1}^{[N/2]} P_{N_1}$, exceeds 80% for $N \geq 8$ (here, [...] stand for the integer part).

Another similarity to the MF is seen in the fact that the quench-produced configuration, being a superposition of multi-string eigenstates with different energies, oscillates in time due to their interference, thus qualitatively resembling the breather. The binding energy of the multi-string solution is the sum of the constituting string energies, each one being $E_{N_1} = -N_1(N_1^2 -$

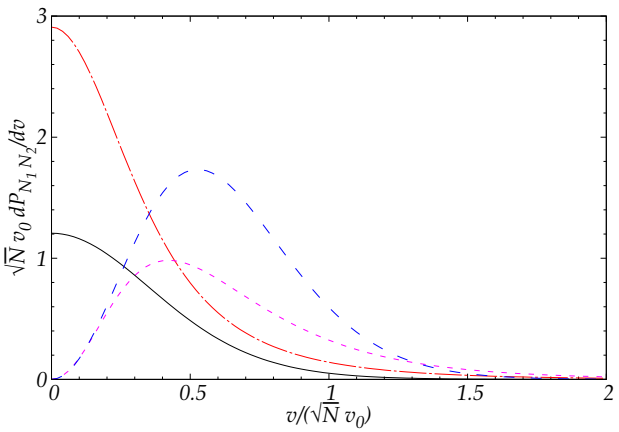

FIG. 1. Channel-selective probability distributions for the relative velocity [see Eq. (2)] of the dissociation products, produced by the application of the quench to the single string (fundamental quantum soliton). The black solid and red dot-dashed lines show $dP_{15,5}/dv$ and $dP_{3,1}/dv$, for $N = 20$ and 4, respectively and the same ratio, $N_1/(N-N_1) = 3:1$, as the MF breather. Plots for other ratios have similar shapes except for ones with $N_1 = N/2$, which are shown by the blue long and magenta short dashes ($10^6 dP_{10,10}/dv$ and $10dP_{2,2}/dv$, respectively). The velocity scale v_0 is defined by Eq. (3).

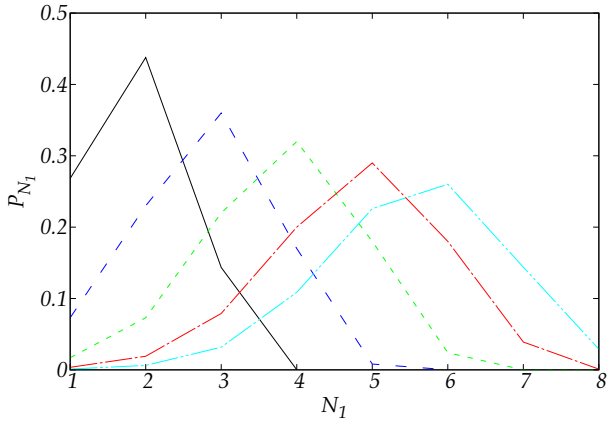

FIG. 2. Total probabilities for different dissociation channels (4), produced by the application of the $g/4 \to g$ quench to the single string (fundamental quantum soliton) composed of $N = 8$, 12, 16, 20, and 23 atoms (black solid, blue long-dashed, green short-dashed, red dot-dashed, and cyan dot-dot-dashed lines, respectively).

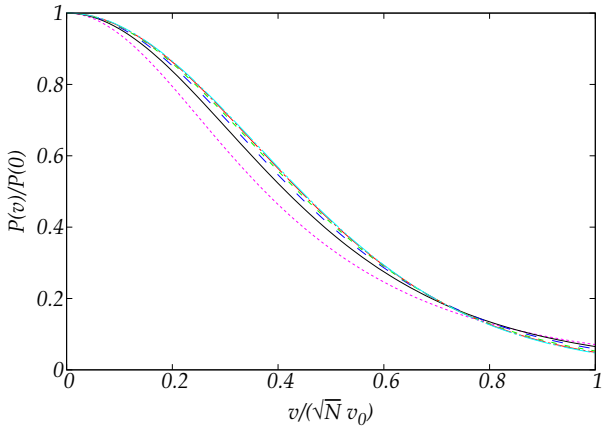

FIG. 3. Probability distributions [see Eq. (5)], totalled over all double-string dissociation channels, for the relative velocity of the emerging strings, as produced by the application of the quench to the single string (fundamental quantum soliton) composed of $N = 4$, 8, 12, 16, 20, and 23 particles (magenta dotted, black solid, blue long-dashed, green short-dashed, red dot-dashed, and cyan dot-dot-dashed lines, respectively, the last three lines are almost indistinguishable). Velocity scale v_0 is taken as per Eq. (3).

$1)mg^2/(24\hbar^2)$ [24, 25]. In particular, the binding-energy difference between the $(N_1, N-N_1)$ and $(N_1-1, N-N_1+1)$ double-string states leads to beatings at frequency $[E_{N_1-1}+E_{N-N_1+1}-(E_{N_1}+E_{N-N_1})]/\hbar = N[N_1-(N+1)/2]mg^2/(4\hbar^3)$, which tends to the the MF breather frequency, $mg^2N^2/(16\hbar^3)$, at $N_1 = 3N/4 \to \infty$.

Probability distributions for the relative velocity of the dissociation products, summed up over all double-string dissociation channels,

$$P(v) = \sum_{N_1=1}^{[N/2]} \frac{dP_{N_1,N-N_1}(v)}{dv}, \tag{5}$$

is almost independent of N, see its plot as a function of $v/\sqrt{N}$ in Fig. 3.

The numerically calculated half-width at half-maximum (HWHM), Δv, of the velocity distribution, defined by $P(\Delta v) = P(0)/2$, can be fitted to the following formula, which is, naturally, close to the $\sqrt{N}$ dependence:

$$\Delta v \approx 0.39 N^{0.54} v_0, \tag{6}$$

see Fig. 4. The relative velocity can be measured also by its mean-square value,

$$\left\langle v^2 \right\rangle = \int_0^\infty v^2 P(v) dv \Big/ \int_0^\infty P(v) dv$$

However, the numerically found root-mean-square (r.m.s.) velocity increases with N only as

$$\sqrt{\left\langle v^2 \right\rangle} \approx 0.63 N^{0.36} v_0, \tag{7}$$

according to the fit displayed in Fig. 4. The probability distribution (2) has slowly decaying tails for small N, in particular, $dP_{3N/4,N/4}(v)/dv \sim v^{-3N}$ at $v \to \infty$. The tails increase the r.m.s. velocity at small N and, therefore, slower its gain with N. On the contrary, due to the normalization condition, the tails exhaust the width of the central part of the v distribution at small N, boosting the HWHM growth with N. Then at large N, when the tail effects fade out, the r.m.s. velocity and HWHM should gain faster and slower, respectively, than at small N. These arguments suggest that both measures of the relative velocity variation assume the same asymptotic scaling at large N, which should be close to $\sqrt{N}$, according to Fig. 3. The eventual fit is displayed in Fig. 4:

$$\Delta v \approx 0.44 \sqrt{N} v_0. \tag{8}$$

The following estimate confirms the $\sqrt{N}$ scaling for a typical relative velocity of the solitons, δv. Consider the system placed in an external harmonic-oscillator (HO) potential with frequency Ω. Varying Ω from vanishingly small values towards very large ones, at each Ω one can apply the $g/4 \to g$ quench to the respective ground state. The figure of merit to monitor is $\delta\tilde{x}$—the time-averaged distance, further symmetrized over permutations, between COMs of two groups of atoms, each containing the number of atoms $\sim N$. At small Ω, the state obtained right after the quench is unaffected by the external confinement, hence the two solitons (strings) start their motion with the free-space relative velocity δv. Thus, the distance $\delta\tilde{x}$ will be dominated by the typical distance between the solitons placed in the HO potential, $\delta v/\Omega$,

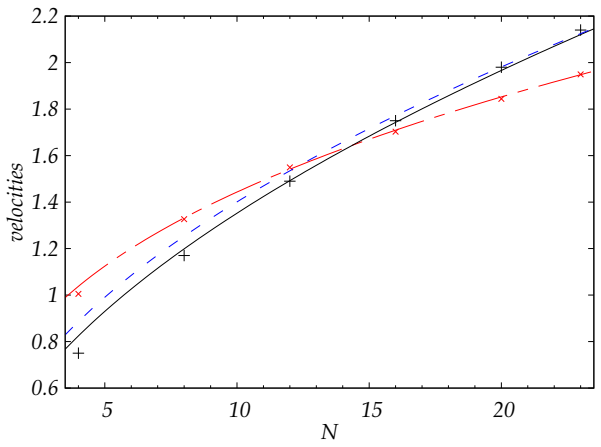

FIG. 4. HWHM (pluses) and r.m.s. (crosses) values of the relative velocity averaged over all double-string (two-soliton) dissociation channels, as a function of the number of atoms, N. Fits provided by Eqs. (6), (7), and (8) are shown by the black solid, red dot-dashed, and blue dashed lines, respectively. The velocity unit is v_0 [see Eq. (3)].

which diverges at small Ω. This very long scale governs the estimate for $\delta\tilde{x}$, the other potentially relevant length scale, the average distance between two atoms inside the same soliton, which is on the order of the size of an individual soliton, $\sim \hbar^2/(m|g|N)$, does not diverge at $\Omega \to 0$. Thus,

$$\delta\tilde{x}_{\Omega\to 0} \sim \delta v/\Omega \ .$$

On the other hand, at large Ω, the effect of the interatomic interactions vanishes and the estimate for $\delta\tilde{x}$ is determined by zero-point quantum fluctuations of the COM position of the cloud containing $\sim N$ particles:

$$\delta\tilde{x}_{\Omega\to\infty} \sim \sqrt{\hbar/(Nm\Omega)} \ .$$

A crossover between the two regimes occurs when the interaction energy per particle (comparable to the chemical potential of the gas, μ), estimated as $\sim \mu \sim mg^2N^2/\hbar^2$, becomes comparable to the HO quantum, $\hbar\Omega$. Indeed, when the former is dominated over by the latter, the interactions are irrelevant, and the system becomes an HO-confined ideal gas. At the crossover, the two above-mentioned estimates yield the same value. An estimate for δv immediately follows:

$$\delta\tilde{x}_{\Omega\to 0}|_{\mu\sim\hbar\Omega} \sim \delta\tilde{x}_{\Omega\to\infty}|_{\mu\sim\hbar\Omega} \ \Rightarrow$$
$$\delta v \sim \sqrt{\frac{\hbar\Omega}{Nm}}\Big|_{\Omega\sim\frac{mg^2N^2}{\hbar^3}} \sim \frac{|g|}{\hbar}\sqrt{N} \ .$$

Indeed, this estimate is consistent with the fit (8).

The above results suggest that experimental observation of the variance in the relative velocity of the solitons due to quantum many-body effects may be possible. To demonstrate this, we consider 3×10^3 ^{7}Li atoms, in a waveguide with transverse trapping frequency $\omega_\perp = 2\pi \times 254$ Hz. The initial state is a fundamental matter-wave soliton, existing at scattering length $a_{t<0} = -1.0\, a_{\rm Bohr}$, which is quenched up to $a_{t>0} = -4\, a_{\rm Bohr}$ [49]. The resulting state constitutes an NLS breather with an aphelion density profile proportional to $\mathrm{sech}^2(x/\ell_{\rm breather})$ and width $\ell_{\rm breather} = 8\hbar^2/(mgN) = 36\ \mu$m [21, 22]. Assuming that the splitting of the breather into two solitons becomes apparent when the distance between their COMs, after evolution time τ, $\Delta x = \Delta v \cdot \tau$, becomes comparable to the breather's width $\ell_{\rm breather}$, and using extrapolation (6) for the relative velocity of the solitons, we obtain $\tau \simeq 3$ s for the time necessary to certainly observe the splitting of the breather caused by the quantum dynamics.

The predicted dissociation time can be made even shorter at the expense of reducing the cloud population, assuming that the scattering length simultaneously increases so as to keep product Na at a finite fraction of the collapse critical value, $Na \lesssim a_\perp$, $a_\perp \sim \sqrt{\hbar/(m\omega_\perp)}$ being the size of the transverse vibrational ground state of the waveguide used. The microscopic velocity scale v_0, the separation velocity Δv, and the breather size $\ell_{\rm breather}$ can be estimated as $v_0 \lesssim \hbar/(ma_\perp N)$, $\Delta v \lesssim \hbar/(ma_\perp\sqrt{N})$, and $\ell_{\rm breather} \gtrsim a_\perp$, respectively. Then the breather dissociation time diminishes as $\tau \sim \ell_{\rm breather}/\Delta v \gtrsim (1/\omega_\perp)\sqrt{N}$ with the decrease of the number of particles.

For the analysis of possibilities for the experimental implementation of the predictions reported here, it is important to estimate deviations of real-world settings from the idealized model [50–52]. In this connection, it is essential to consider the departure from the one-dimensionality, as suggested, in particular, by the work aimed at experimental observation of the quantum violation of the scale-invariance-induced constancy of the monopole-mode frequency in the 2D Bose gas. In that case, weak dependence of the quantum state on the third, confined dimension tends to mask the quantum many-body effects [53]. Nevertheless, experiments have clearly demonstrated that 3D experimental setups with appropriately designed transverse confinement can be efficiently used for the emulation of ideal one-dimensional quantum settings, and such emulations are stable against real-world disturbances. Relevant examples are the creation of the atomic Newton's cradle with repulsive interactions [54], and the realization of the super-Tonks-Girardeau gas [55]. The latter example is especially relevant for the comparison with the present analysis, as it is also based on attractive interactions. Predictions of the MF counterpart of the Lieb-Liniger model, i.e., the Gross-Pitaevskii equation, which are also based on the one-dimensionality and integrability, are very well confirmed in numerous experiments with matter-wave solitons [56–60]. The well-known stability of the exact solution of the Lieb-Liniger model [24, 42] clearly means that the results may only be slightly perturbed by other distortions, such as external

fluctuations and inhomogeneities.

As concerns the full 3D analysis, an example which makes it possible to explicitly compare the MF approximation and its many-body counterpart is offered by the problem of the stabilization of the gas of bosons with repulsive interactions, attracted to the center with potential $\sim -r^{-2}$. In that case, the MF predicts suppression of the quantum collapse and creation of a ground state which is missing in the single-particle formulation [61], while the full many-body analysis demonstrates that the same newly created state exists as a metastable one [62].

To summarize, we have showed that the dissociation of the 1D matter-wave breather, initiated by the quench from the fundamental soliton, is a purely quantum many-body effect, as all the MF contributions to the dissociation vanish due to the integrability at the MF level. This conclusion opens the way to observe truly quantum many-body effects without leaving the MF range of experimental parameters. We have evaluated the dissociation time corresponding to typical experimental parameters for atomic solitons. The extrapolation of the present results to a larger number of atoms is justified [46] by the comparison with recent results produced by truncated Wigner calculations in Ref. [63] (that work has appeared after the submission of the first version of the present one).

We acknowledge financial support provided jointly by the National Science Foundation, through grants PHY-1402249, PHY-1408309, PHY-1607215, and PHY-1607221, and Binational (US-Israel) Science Foundation through grant No. 2015616, as well as support from the Welch Foundation (grant C-1133), the Army Research Office Multidisciplinary University Research Initiative (grant W911NF-14-1-0003), and the Office of Naval Research. We thank L. D. Carr, P. Drummond, V. Dunjko, and C. Weiss for valuable discussions.

* volodia@post.tau.ac.il

[1] T. Kinoshita, T. Wenger, and D. S. Weiss, Science **305**, 1125 (2004).
[2] B. Laburthe Tolra, K. M. O'Hara, J. H. Huckans, W. D. Phillips, S. L. Rolston, and J. V. Porto, Phys. Rev. Lett. **92**, 190401 (2004).
[3] N. Navon, S. Piatecki, K. Günter, B. Rem, T. C. Nguyen, F. Chevy, W. Krauth, and C. Salomon, Phys. Rev. Lett. **107**, 135301 (2011).
[4] I. Ferrier-Barbut, H. Kadau, M. Schmitt, M. Wenzel, and T. Pfau, Phys. Rev. Lett. **116**, 215301 (2016).
[5] M. Schmitt, M. Wenzel, F. Boettcher, I. Ferrier-Barbut, and T. Pfau, Nature **539**, 259 (2016).
[6] L. Chomaz, S. Baier, D. Petter, M. J. Mark, F. Wächtler, L. Santos, and F. Ferlaino, Phys. Rev. X **6**, 041039 (2016).
[7] C. R. Cabrera, L. Tanzi, J. Sanz, B. Naylor, P. Thomas, P. Cheiney, and L. Tarruell, arXiv:1708.07806 (2017).
[8] D. S. Petrov, Phys. Rev. Lett. **115**, 155302 (2015).
[9] D. S. Petrov and G. E. Astrakharchik, Phys. Rev. Lett. **117**, 100401 (2016).
[10] D. Baillie, R. M. Wilson, R. N. Bisset, and P. B. Blakie, Phys. Rev. A **94**, 021602 (2016).
[11] C. A. Sackett, J. M. Gerton, M. Welling, and R. G. Hulet, Phys. Rev. Lett. **82**, 876 (1999).
[12] J. M. Gerton, D. Strekalov, I. Prodan, and R. G. Hulet, Nature **408**, 692 (2000).
[13] E. Donley, N. Claussen, S. Cornish, J. Roberts, E. Cornell, and C. Wieman, Nature **412**, 295 (2001).
[14] J. M. Vogels, K. Xu, and W. Ketterle, Phys. Rev. Lett. **89**, 020401 (2002).
[15] J. K. Chin, J. M. Vogels, and W. Ketterle, Phys. Rev. Lett. **90**, 160405 (2003).
[16] V. A. Yurovsky, Phys. Rev. A **65**, 033605 (2002).
[17] V. I. Yukalov and E. P. Yukalova, Laser Physics Letters **1**, 50 (2004).
[18] M. Olshanii, H. Perrin, and V. Lorent, Phys. Rev. Lett. **105**, 095302 (2010).
[19] K. S. Gupta and S. G. Rajeev, Phys. Rev. D **48**, 5940 (1993).
[20] M. J. Ablowitz and H. Segur, *Solitons and the Inverse Scattering Transform* (SIAM, Philadelphia, 1981).
[21] V. E. Zakharov and A. B. Shabat, Soviet Physics JETP **34**, 62 (1972).
[22] J. Satsuma and N. Yajima, Supp. Progr. Theor. Phys. **55**, 284 (1974).
[23] L. D. Carr and Y. Castin, Phys. Rev. A **66**, 063602 (2002).
[24] F. A. Berezin, G. P. Pohil, and V. M. Finkelberg, Vestnik Moskovskogo Universiteta (in Russian) **No. 1**, 21 (1964).
[25] J. B. McGuire, J. Math. Phys. **5**, 622 (1964).
[26] F. Calogero and A. Degasperis, Phys. Rev. A **11**, 265 (1975).
[27] Y. Lai and H. A. Haus, Phys. Rev. A **40**, 854 (1989).
[28] Y. Lai and H. A. Haus, Phys. Rev. A **40**, 844 (1989).
[29] S. J. Carter, P. D. Drummond, M. D. Reid, and R. M. Shelby, Phys. Rev. Lett. **58**, 1841 (1987).
[30] P. D. Drummond and S. J. Carter, J. Opt. Soc. Am. B **4**, 1565 (1987).
[31] M. Rosenbluh and R. M. Shelby, Phys. Rev. Lett. **66**, 153 (1991).
[32] P. Drummond, R. Shelby, S. Friberg, and Y. Yamamoto, Nature **365**, 307 (1993).
[33] J. F. Corney, P. D. Drummond, J. Heersink, V. Josse, G. Leuchs, and U. L. Andersen, Phys. Rev. Lett. **97**, 023606 (2006).
[34] J. F. Corney, J. Heersink, R. Dong, V. Josse, P. D. Drummond, G. Leuchs, and U. L. Andersen, Phys. Rev. A **78**, 023831 (2008).
[35] P. Drummond and S. Chaturvedi, Physica Scripta **91**, 073007 (2016).
[36] P. Drummond and W. Man, Optics Communications **105**, 99 (1994).
[37] T. Vaughan, P. Drummond, and G. Leuchs, Phys. Rev. A **75**, 033617 (2007).
[38] Y. Castin, Eur. Phys. J. B **68**, 317 (2009).
[39] C. Weiss and L. D. Carr, "Higher-order quantum bright solitons in Bose-Einstein condensates show truly quantum emergent behavior," Preprint at arXiv:1612.05545 (2016).
[40] M. Olshanii, Phys. Rev. Lett. **81**, 938 (1998).
[41] V. A. Yurovsky, M. Olshanii, and D. S. Weiss, in *Adv.*

At. Mol. Opt. Phys., Vol. 55 (Elsevier Academic, New York, 2008) p. 61.
[42] E. H. Lieb and W. Liniger, Phys. Rev. **130**, 1605 (1963).
[43] C. N. Yang, Phys. Rev. **168**, 1920 (1968).
[44] Z. Wang, J. Wu, W. Yang, A. K. Bera, D. Kamenskyi, A. T. M. N. Islam, S. Xu, J. M. Law, B. Lake, and C. Wu, "Experimental observation of Bethe strings," Preprint at arXiv:1706.04181 (2017).
[45] P. Calabrese and J.-S. Caux, Phys. Rev. Lett. **98**, 150403 (2007).
[46] See Supplemental Material for derivation details, which includes Refs. [47, 48].
[47] "Maxima, a computer algebra system," `http://maxima.sourceforge.net/`.
[48] J. P. Gordon, Opt. Lett. **8**, 596 (1983).
[49] For the present set of parameters, the number of atoms is only two times lower than the collapse critical number, $N_{\rm crit} = 7900$, hence deviations from the purely 1D behavior are expected. However, moderate 3D corrections do not destroy MF breathers [64].
[50] Y. S. Kivshar and B. A. Malomed, Rev. Mod. Phys. **61**, 763 (1989).
[51] H. Sakaguchi and B. A. Malomed, Phys. Rev. E **70**, 066613 (2004).
[52] H. Yanay, L. Khaykovich, and B. A. Malomed, Chaos **19**, 033145 (2009).
[53] K. Merloti, R. Dubessy, L. Longchambon, A. Perrin, P.-E. Pottie, V. Lorent, and H. Perrin, New Journal of Physics **15**, 033007 (2013).
[54] T. Kinoshita, T. Wenger, and D. S. Weiss, Nature **440**, 900 (2006).
[55] E. Haller, M. Gustavsson, M. Mark, J. Danzl, R. Hart, G. Pupillo, and H.-C. Nägerl, Science **325**, 1224 (2009).
[56] K. E. Strecker, G. B. Partridge, A. G. Truscott, and R. G. Hulet, Nature **417**, 150 (2002).
[57] L. Khaykovich, F. Schreck, G. Ferrari, T. Bourdel, J. Cubizolles, L. D. Carr, Y. Castin, and C. Salomon, Science **296**, 1290 (2002).
[58] A. L. Marchant, T. P. Billam, T. P. Wilses, M. M. H. Yu, S. A. Gardiner, and S. L. Cornish, Nature Comm. **4**, 1865 (2013).
[59] J. H. V. Nguyen, P. Dyke, D. Luo, B. A. Malomed, and R. G. Hulet, Nat. Phys. **10**, 918 (2014).
[60] A. L. Marchant, T. P. Billam, M. M. H. Yu, A. Rakonjac, J. L. Helm, J. Polo, C. Weiss, S. A. Gardiner, and S. L. Cornish, Phys. Rev. A **93**, 021604(R) (2016).
[61] H. Sakaguchi and B. A. Malomed, Phys. Rev. A **83**, 013607 (2011).
[62] G. E. Astrakharchik and B. A. Malomed, Phys. Rev. A **92**, 043632 (2015).
[63] B. Opanchuk and P. D. Drummond, "One-dimensional Bose gas dynamics: breather relaxation," Preprint at arXiv:1708.01013 (2017).
[64] J. Golde, J. Ruhl, B. A. Malomed, M. Olshanii, and V. Dunjko, "Metastability versus collapse following a quench in attractive Bose-Einstein condensates," Preprint at arXiv:1706.07096 (2017).